Arch. Mech., **54**, 1, pp. 75–91, Warszawa 2002

Deformation behavior of TiNi shape-memory alloy under strain- or stress-controlled conditions

H. TOBUSHI [1], K. OKUMARA [1], M. ENDO [1] and K. TANAKA [2]

[1] *Department of Mechanical Engineering,*
Aichi Institute of Technology
1247 Yachigusa, Yagusa-cho, Toyota 470-0392, Japan
e-mail : tobushi@me.aitech.ac.jp

[2] *Department of Aerospace Engineering,*
Tokyo Metropolitan Institute of Technology
Asahigaoka 6-6, Hino, Tokyo, 191-0065, Japan

THE DEFORMATION PROPERTIES of TiNi shape-memory alloy subjected to strain control and stress control were investigated experimentally. The results obtained are summarized as follows. (1) In the case of a full loop, the stress-strain curves under stress-controlled conditions are similar to those under strain-controlled conditions with high strain rate. The overshoot and undershoot do not appear at the start points of the stress-induced martensitic transformation in these curves. (2) In the case of subloop under stress-controlled conditions, temperature decreases and therefore the strain increases owing to the martensitic transformation at the early stage of the unloading process. At the early stage in the reloading process, temperature increases and therefore the strain decreases owing to the reverse transformation. (3) In the case of subloop under stress-controlled conditions, the starting stresses of the martensitic transformation and the reverse transformation in the loading and unloading processes coincide with the transformation stresses under strain-controlled conditions with low strain rate, respectively. (4) The deformation behaviours for a subloop under stress-controlled conditions are prescribed by the condition for progress of the martensitic transformation based on the transformation kinetics. (5) The deformation behaviors subjected to cyclic loading under stress-controlled conditions at constant temperature are also prescribed by the conditions for progress of the martensitic transformation.

Key words: Shape Memory Alloy, Titanium-Nickel Alloy, Stress-Induced Martensitic Transformation, Superelasticity, Strain-Controlled Conditions, Stress-Controlled Conditions, Subloop, Transformation Kinetics

1. Introduction

IN A SHAPE-MEMORY alloy (SMA), the shape-memory effect (SME) and superelasticity (SE) appear [1-4]. The strain of 6-8% is recovered by heating in SME and is recovered by unloading in SE. In both cases, strain appears owing to the stress-induced martensitic transformation (SIMT) in the loading process and disappears due to the reverse transformation by heating or unloading.

The recovery stress and recovery strain of SMA which appear due to SIMT are applied to working elements of actuators, robots and solid-state heat engines. In these applications of SMA, the deformation properties of the material are important. The deformation properties due to SIMT vary, depending on temperature and strain rate [5-6]. The basic deformation modes are strain-controlled and stress-controlled conditions. The difference in deformation behaviors between both conditions was reported recently [7]. Most deformation behaviors have been investigated under strain-controlled conditions till now, but few behaviors under the stress-controlled conditions. In the case of subloop under stress-controlled conditions, the SIMT starting stress in the subsequent reloading process does not coincide with the stress from which partial unloading started [7]. In the case of strain variation during SIMT, the thermomechanical state varies due to SIMT. Therefore the progress of deformation due to SIMT cannot be prescribed only by the mechanical condition. Since SMA elements work repeatedly, the cyclic deformation properties of SMA are particularly important [8-9].

In the present study, by the tensile test under strain-controlled and stress-controlled conditions, the deformation behaviours of TiNi SMA subjected to various strain rates, cyclic loading and various strain variations are investigated. The thermomechanical condition for the progress of SIMT is discussed basing on the constitutive equation of the material. The difference in deformation behavior between strain-controlled condition and stress-controlled condition is considered. The subsequent strain variation after cyclic deformation is discussed.

2. Condition for progress of martensitic transformation

In the present study, the deformation behavior of SMA due to martensitic transformation (MT) is discussed basing on the condition for progress of MT. The constitutive relationships proposed by Tanaka [10, 11] are as follows. The constitutive equation is

$$\dot{\sigma} = D\dot{\varepsilon} + \Theta\dot{T} + \Omega\dot{\xi} \tag{2.1}$$

and the transformation kinetics for the MT is

$$\frac{\dot{\xi}}{1-\xi} = b_M C_M \dot{T} - b_M \dot{\sigma} \geq 0 \tag{2.2}$$

or, for the reverse transformation,

$$-\frac{\dot{\xi}}{\xi} = b_A C_A \dot{T} - b_A \dot{\sigma} \geq 0 \tag{2.3}$$

where σ, ε and T represent the stress, strain and temperature, respectively. The coefficients D and Θ represent the modulus of elasticity and the thermoelastic constant, respectively. ξ represents the volume fraction of the martensitic (M) phase. Therefore, volume fraction of the parent phase is 1–ξ. The dot over the symbol denotes the time derivative. The material parameters b_M, C_M, b_A and C_A are determined from expriments. Equation (2.2) is applied to the MT and Eq. (2.3) to the reverse transformation.

If these equations are integrated by assuming these parameters to be constant, Eq. (2.2) and Eq. (2.3) become respectively as follows:

$$\xi = 1 - \exp\{b_M C_M (Ms - T) + b_M \sigma\}, \tag{2.4}$$

$$\xi = \exp\{b_A C_A (As - T) + b_A \sigma\}, \tag{2.5}$$

where M_S and A_S stand for the temperatures at which the MT and the reverse transformation start under the stress-free conditions. From Eq. (2.4), the MT starting and completing lines become as follows:

$$\sigma = C_M (T - M_s), \tag{2.6}$$

$$\sigma = C_M (T - M_s) - 2 \ln 10 / b_M, \tag{2.7}$$

and are expressed by the straight lines with a slope of C_M. From Eq. (2.5) the reverse-transformation starting and completing lines become as follows:

$$\sigma = C_A (T - A_s), \tag{2.8}$$

$$\sigma = C_A (T - A_s) - 2 \ln 10 / b_A, \tag{2.9}$$

and are expressed by the straight lines with a slope of C_A. On deriving Eqs. (2.7) and (2.9) we have assumed that the transformation is completed when the fraction of induced phase reaches 0.99. The transformation lines and the transformation region are prescribed by Eqs. (2.6)-(2.9). If they are drawn on the stress-temperature plane shown in Fig. 1, Eqs. (2.6)-(2.9) are expressed respectively by the straight lines M_S, M_F, A_S and A_F, and each transformation progresses in the transformation strip between the starting line and the completing line.

From Eq. (2.2), the condition for progress of the MT becomes as follows:

$$b_M C_M \dot{T} \geq b_M \dot{\sigma}, \quad b_M < 0$$

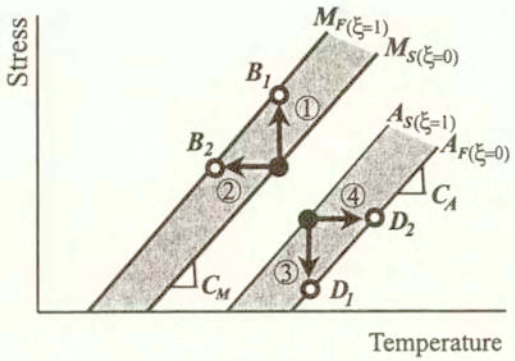

FIG. 1. Transformation lines.

and therefore

$$\begin{aligned} &\frac{d\sigma}{dT} \geq C_M \quad \text{for} \quad dT > 0, \\ &\frac{d\sigma}{dT} \leq C_M \quad \text{for} \quad dT < 0. \end{aligned} \tag{2.10}$$

From Eq. (2.3), the condition for progress of the reverse transformation becomes as follows:

$$b_A C_A \dot{T} \geq b_A \dot{\sigma}, \quad b_A > 0$$

and therefore

$$\begin{aligned} &\frac{d\sigma}{dT} \leq C_A \quad \text{for} \quad dT > 0, \\ &\frac{d\sigma}{dT} \geq C_A \quad \text{for} \quad dT < 0. \end{aligned} \tag{2.11}$$

The MT progresses if the condition (2.10) is satisfied and the reverse transformation progresses if the condition (2.11) is satisfied. Both transformations progress in the transformation strips which are shadowed on the stress-temperature plane in Fig. 1. For example, in the case of loading or unloading from points A or C at constant temperature, the loading path ① or unloading path ③ satisfies the conditions (2.10) or (2.11) and each transformation progresses along the path. In the case of heating or cooling under constant stress, the MT progresses along the cooling path ② and the reverse transformation along the heating path ④.

The conditions for progress of the phase transformation in the subloop during the phase transformation are shown in Fig. 2. The points A and C in Fig. 2(a)

represent respectively the progressing state of the MT and the reverse transformation, and the volume fractions of the M-phase at each point are ξ_A and ξ_C. The dashed lines M_m and A_m denote the states with the volume fractions ξ_A and ξ_C, respectively. The conditions for progress of the transformation prescribed by Eq. (2.10) and Eq. (2.11) mean that stress and temperature vary from the points A and C to the directions shown by the arrows in Fig. 2(a).

The conditions for progress and stop of the subsequent transformation are shown in Fig. 2(b). In Fig. 2(b), the MT progress in the loading path ① and unloading path ② and stops in the unloading path ③. The reverse transformation progresses in the unloading path ④ and loading path ⑤ and stops in the loading path ⑥.

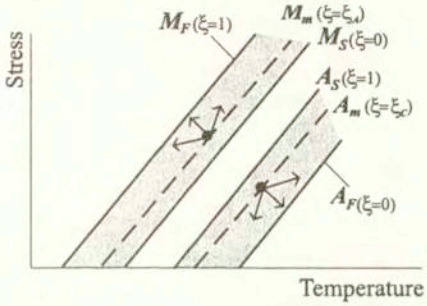

(a) Path for progress of phase transformation

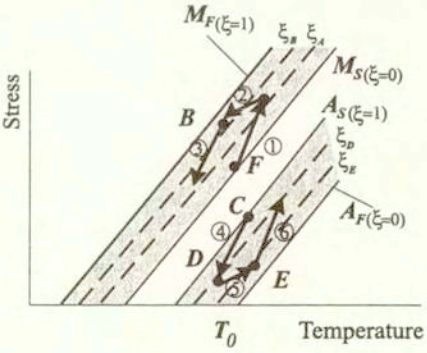

(b) Path for progress and stop pf phase transformation

FIG. 2. Conditions for progress of phase transformation in the subloop during phase transformation.

3. Experimental method

3.1. Materials and specimen

The material was a Ti-55.4wt%Ni SMA wire, 0.75mm in diameter. The specimens were given the shape memory of a straight line through shape memory processing. This was carried out by holding the wires in the straight line at 673K for 60 min and then cooling in a furnace. The specimens were straight lines with uniform cross-sections. The reverse-transformation completion temperature A_f was about 323K.

3.2. Experimental apparatus

The experimental apparatus was an SMA property testing machine composed of a tensile machine and a heating-cooling device [12]. Temperature was measured with a thermocouple, 0.1mm in diameter, on the surface in the central part of the specimens. Displacement and load were measured with an extensometer of 20mm gauge length and a load cell, respectively.

3.3. Experimental procedure

The following five experiments were performed.

1. Exp. I: Dependence on the rate
   Tensile tests under constant rate were carried out at test temperature $T_0 = 353$K for maximum strain $\varepsilon_m = 8\%$. Strain rates $\dot{\varepsilon}$ were 1 and 10%/min, and stress rates $\dot{\sigma}$ were 1 and 10MPa/s.
2. Exp. II: Cyclic full-loop behavior
   Loading, and unloading were repeated 100 times at test temperature $T_0 = 353$K for maximum strain $\varepsilon_m = 8\%$. Strain rate $\dot{\varepsilon}$ was 1%/min and stress rate $\dot{\sigma}$ was 30MPa/s.
3. Exp. III: Subloop behavior
   Loading and unloading under subloop were carried out at test temperature $T_0 = 353$K. Strain rate $\dot{\varepsilon}$ was 10%/min and stress rates $\dot{\sigma}$ were 1, 10 and 30MPa/s.
4. Exp. IV: Cyclic subloop behavior
   Loading to the strain $\varepsilon_1 = 4\%$ and subsequent unloading to the strain $\varepsilon_2 = 1\%$ were repeated seven times at test temperature $T_0 = 353$K. After the cyclic deformation, loading to the maximum strain $\varepsilon_m = 8\%$ was performed. Stress rate $\dot{\sigma}$ was 30MPa/s.
5. Exp. V: Subloop behavior after cyclic deformation
   After cyclic deformation to maximum strain $\varepsilon_m = 8\%$ (100 times), loading and unloading under subloop were performed at the test temperature $T_0 = 353$K. Stress rates were 1 and 30MPa/s.

4. Experimental results and discussion

In performing the experiment and dealing with the experimental data, stress and strain were treated in terms of nominal stress and nominal strain, respectively. Therefore the stress-controlled and strain-controlled conditions mean the load-controlled and displacement-controlled conditions, respectively.

4.1. Deformation behavior under strain- and stress-controlled conditions

In order to investigate the dependence of SIMT on the rate under strain-controlled and stress-controlled conditions, Exp. I was performed. The stress-strain curves obtained by Exp. I are shown in Fig. 3.

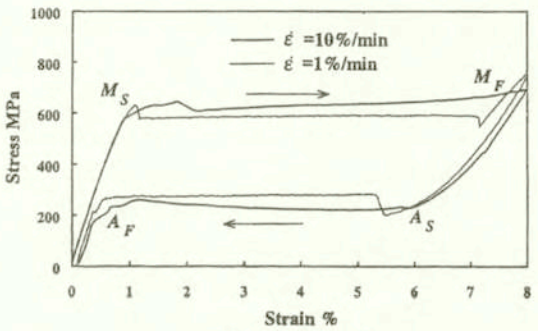

(a) Strain-controlled

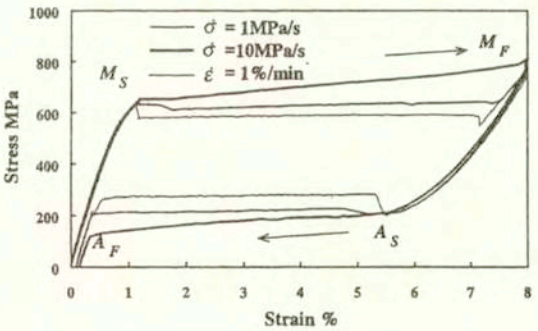

(b) Stress-controlled and strain-controlled

FIG. 3. Stress-strain curves under various strain rates and stress rates.

As seen in Fig. 3(a), in the case of low strain rate $\dot{\varepsilon}$ under strain-controlled condition, an overshoot appears at the point M_s and an undershoot at the point A_s. On the other hand, in the case of high strain rate, the overshoot and undershoot do not appear. In the case of low strain rate, the interface between the M-phase

and the parent phase moves under constant stresses which are expressed by stress plateaus following the points M_s and A_s. At the points M_s and A_s, an excessive energy is necessary to create a nucleus of the induced phase compared with the movement of the interface, and therefore an overshoot and an undershoot appear. The MT is exothermic and the reverse transformation is endothermic. In the case of low strain rate, heat generated by SIMT in the interface is radiated and therefore the temperature does not increase. On the contrary, in the case of high strain rate, because the interface at the temperature increased by SIMT moves, temperature of the material increases during the MT and therefore the MT stress increases. In the case of reverse transformation, the higher the strain rate, the larger is the decrease in temperature, resulting in decrease in the transformation stress. Basing on these reasons, the overshoot and undershoot do not appear in the case of high strain rate.

As it is seen in Fig. 3(b), both the overshoot and undershoot do not appear under the stress-controlled condition. This is due to the stress-controlled condition that stress increases in the loading process and decreases in the unloading process. In this case, the MT and the reverse transformation start respectively under the same stresses as those at the starting points M_s and A_s for a low strain rate. Because the amount of variation in stress is small in the transformation region, the deformation (strain) rate becomes high, resulting in the same deformation behavior as that under high strain rate.

4.2. Cyclic deformation property

The stress-strain curves obtained by Exp. II are shown in Fig. 4. The curves are parameterized by the number of cycles N. As it can be seen in Fig. 4(a) for the strain-controlled conditions, the MT stress decreases and residual strain increases with an increase in N. Both the rate of decrease in the MT stress and the rate of increase in residual strain decrease with an increase in N. The MT stress and residual strain have the inclination to satulate a certain value. It is ascertained by the previous study [13] under strain-controlled condition that dislocations accumulate around the infinitesimal defects in the material with cyclic deformation and both the internal stress and residual strain appear. These cyclic deformation properties under strain-controlled condition are also observed in the case of stress-controlled condition, as shown in Fig. 4(b). In the case of strain-controlled condition, both the overshoot and undershoot diminishes with an increase in N. Therefore, after a certain number of cycles, the deformation behavior under the stress-controlled condition becomes similar as that under the strain-controlled condition [14] except for the difference in the slope of the stress-strain curve in the transformation region.

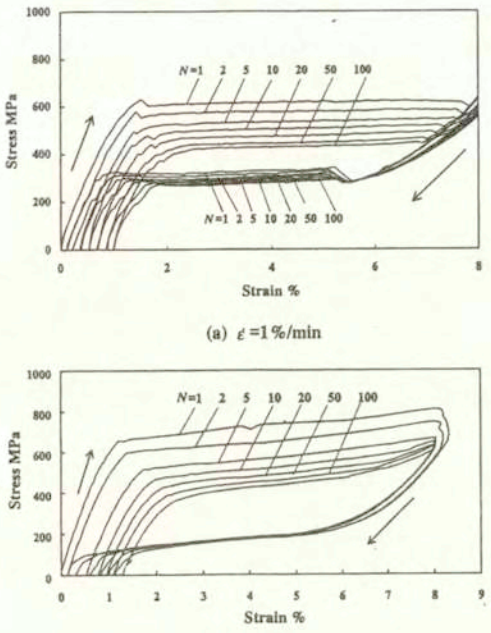

FIG. 4. Stress-strain curves under cyclic loading.

4.3. Deformation behavior in subloop

4.3.1. Deformation behavior under strain-controlled conditions. The stress-strain curves obtained by Exp. III under strain-controlled conditions are shown in Fig. 5. In Fig. 5, the path from point A_i to point D_i denotes the unloading process and the path from point D_i to point $A_{i+1}-$ the reloading process. As seen in Fig. 5, in the unloading process, strain decreases owing to elastic deformation between the points A_i and C_i, and owing to the reverse transformation between the points C_i and D_i. In the reloading process, strain increases owing to elastic deformation between the points D_i and F_i, and owing to the MT between the points F_i and A_{i+1}. The stress σ_A at the start points C_1 and C_2 of the reverse transformation coincides with the stress of the plateau in N=1 under strain rate $\dot{\varepsilon}$=1%/min. The stress σ_M at the start points F_1 and F_2 of the MT coincides with the stress of the plateau in N=2 under $\dot{\varepsilon}$=1%/min. Therefore the starting stresses of the MT and the reverse transformation in the subloop are prescribed by the transformation stresses under low strain rate. In the case of unloading from a point A_1, stress returns to the point A_1 and the MT progresses on the curve which is extended from the initial loading curve. This phenomenon appears as follows. In the initial

loading, the MT progresses to the region which corresponds to the point A_1. In the reloading after the point A_1, the MT progresses in the non-transformed region under the stress level in N=1. The SIMT starting stress in the subsequent reloading process coincides with the stress from which partial unloading starts in the case of low strain rate [15]. This phenomenon is pointed out as the return-point memory effect [7] and is observed for plastic deformation.

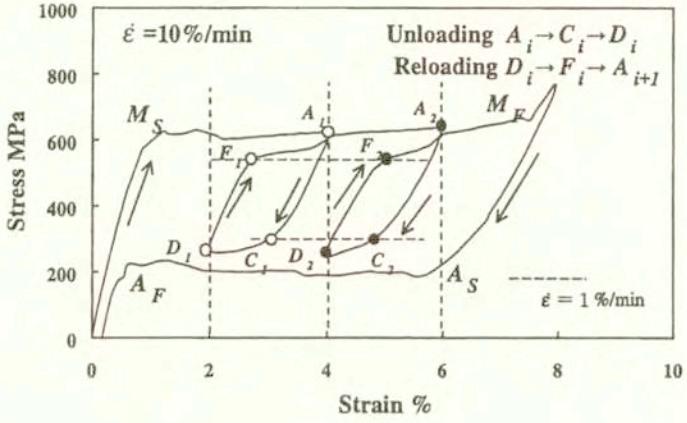

FIG. 5. Stress-strain curves for subloop under strain-controlled conditions.

4.3.2. Deformation behavior under stress-controlled conditions. The stress-strain curves obtained by Exp. III under stress-controlled condition are shown in Fig. 6. In Fig. 6, the path from a point A_i to a point D_i denotes the unloading process and the path from a point D_i to A_{i+1}– the reloading process. As seen in Fig. 6, in the unloading process of the subloop, strain increases between the points A_i and B_i and decreases owing to elastic deformation between the points B_i and C_i, and the curve between the points C_i and D_i is almost parallel to the reverse transformation curve in full loop. The smaller is the strain at a point A_i and the lower is the stress rate $\dot{\sigma}$, the larger will be the amount of strain increment between the points A_i and B_i. In the reloading process, strain decreases between the points D_i and E_i and increases owing to elastic deformation between the points E_i and F_i, and the curve between the points F_i and A_{i+1} is almost parallel to the initial MT curve. The stresses at a point F_1 and a point F_2 do not depend on $\dot{\sigma}$ and are equal to the stress σ_M of the MT plateau in N=2 under the strain-controlled conditions with a low strain rate. The stresses at a point C_1 and a point C_2 do not depend on $\dot{\sigma}$ and are equal the stress σ_A of the reverse transformation plateau under strain-controlled condition with low strain rate.

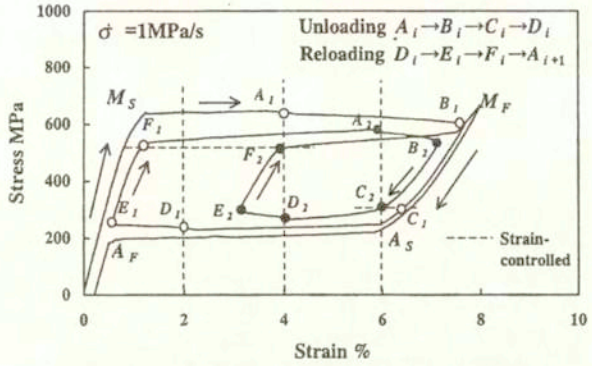

(a) $\dot{\sigma}$ =1MPa/s

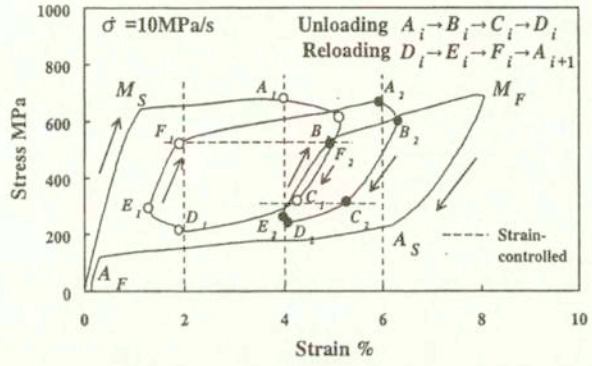

(b) $\dot{\sigma}$ =10MPa/s

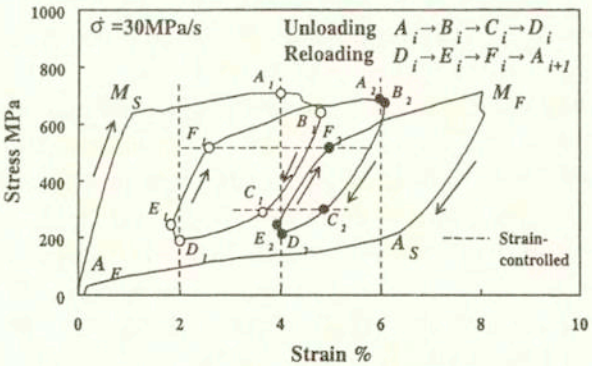

(c) $\dot{\sigma}$ =30MPa/s

FIG. 6. Stress-strain curves for subloop under stress-controlled conditions.

The variation in temperature during subloop under $\dot{\sigma}$=1MPa/s in Exp. III is shown in Fig. 7. In Fig. 7, the abscissa axis expresses the accumulated strain path S. S is determined by the following equation:

$$S = \int |d\varepsilon/dt|\, dt \tag{4.1}$$

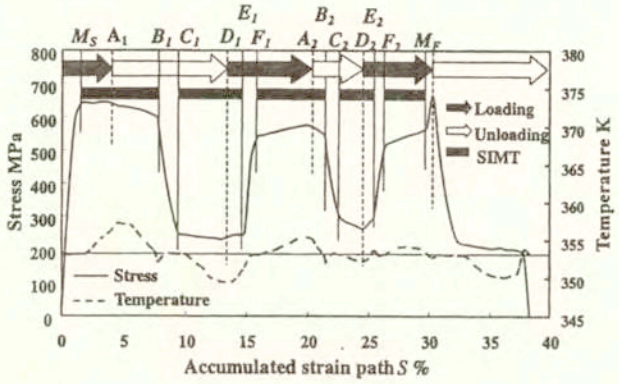

FIG. 7. Temperature variation for subloop under stress-controlled conditions.

where t denotes time. In Fig. 7, variation in stress is shown simultaneously. The symbols $A_i \sim F_i$ in Fig. 7 correspond to those in Fig. 6. As seen in Fig. 7, temperature increases between the points F_i and A_{i+1} in the loading process, decreases between the points A_i and B_i in the unloading process and returns to the ambent temperature at point B_i. Temperature decreases between the points C_i and D_i in the unloading process, increases between the points D_i and E_i in the loading process and returns to the ambient temperature at point E_i. Temperature does not vary during elastic deformation. Temperature variation ΔT from a point A_1 to a point B_1 is –4K. From the experiment performed under various strain rates, temperature rise measured with a thermocouple pressed on the surface of a wire, 0.75mm in diameter, is about 4K [6], and the temperature rise on the surface of a ribbon measured with an infrared thermograph is about 20K [16]. Therefore, the actual temperature variation ΔT from point A_1 to point B_1 is about –20K. Stress variation $\Delta\sigma$ from point A_1 to point B_1 is –35MPa. The slope of the MT line C_M of TiNi SMA is 6.13MPa/K. Therefore the condition for progress of MT prescribed by Eq. (2.10) is satisfied between the points A_1 and B_1. From this fact it follows that MT progresses and strain increases between the points A_1 and B_1 in the unloading process. In the similar manner, from Eqs. (2.10) and (211) which prescribe the condition for progress of MT and the reverse transformaton,

it follows that MT progresses between the points F_i and A_{i+1} and between the points A_i and B_i, and the reverse transformation progresses between the points C_i and D_i and between the points D_i and E_i.

Basing on the above-mentioned discussion, the path under the stress-controlled condition on the stress-temperature plane is shown in Fig. 8.

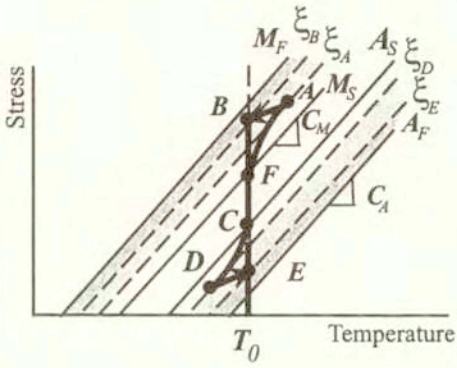

FIG. 8. Stress-temperature path in subloop under stress-controlled conditions.

The symbols A ~F in Fig. 8 correspond to those in Figs. 2, 6 and 7. As seen from Figs. 2, 6, 7 and 8, MT starts at the point M_s and progresses to the point B_1 in the unloading process through the unloading start point A_1. The reverse transformation starts at the point C_1 and progresses to the point E_1 through the reloading start point D_1. Because MT in the loading process between the points M_s and A_1, the points F_1 and A_2 and the points F_2 and M_F is the exothermic transformation, temperature of the material increases. In the unloading process between the points A_i and B_i, because temperature increased owing to MT in the loading process returns to the ambient temperature, temperature of the material decreases. According to the decrease in temperature, MT progresses to the point B_i. Because the reverse transformation in the unloading process between the points C_i and D_i and the points A_s and A_F is the endothermic transformation, temperature of the material decreases. In the reloading process from the point D_i, because temperature decreased owing to the reverse transformation in the unloading process returns to ambient temperature, temperature of the material increases, resulting in progress of the reverse transformation to the point E_i.

As seen in Fig. 6, the higher is the stress rate $\dot{\sigma}$, the smaller will be the amount of variation in transformation strain between the points A_i and B_i and the point D_i and E_i. This phenomenon appears according to the difference in the time necessary to reach the transformation stop points B_i and E_i depending on $\dot{\sigma}$. In the case of high $\dot{\sigma}$, because the time necessary to reach the transformation stop points B_i and E_i is short, the strain transformed during this time is small.

As seen in Fig. 6, strain increment between the points A_1 and B_1 is larger than that between the points A_2 and B_2. This phenomenon appears according to the difference in volume fraction of the M-phase at the point A_i. As found from Eq. (2.2), the smaller is the volume fraction of the M-phase ξ, the larger will be the amount of variation in ξ. The fraction at the point A_1 with strain of 4% is smaller than that at the point A_2 with strain of 6%. Therefore the amount of variation in ξ from the point A_1 is larger than that from A_2, and larger transformation strain increment appears.

4.3.3. Cyclic property. The stress-strain curves obtained by Exp. IV under cyclic subloop are shown in Fig. 9. In Fig. 9, the thin curve expresses the full loop in $N=1$ under strain rate $\dot{\varepsilon}=1\%/\text{min}$. The thin dashed line shows the stress at the

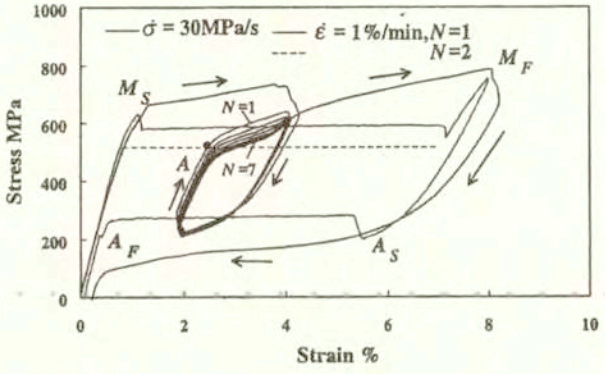

FIG. 9. Stress-strain curves for cyclic subloop.

MT plateau in $N=2$ under the same strain rate. The stress at the MT start point A in the reloading process is equal to the MT stress in $N=2$ under low strain rate. At the initial MT start point M_s, high stress is necessary to create a nucleus of the M-phase in the parent phase. In the case of subloop, MT progresses under stress which is lower than that in the case of initial creation of a nucleus. Because the M-phase exists in the material during the subloop, MT starts under the stress in the case of low strain rate. The MT stress decreases with repeating cycles. Compared with Exp. II under cyclic full loop shown in Fig. 4, the amount of decrease in the MT stress under cyclic subloop is small. This occurs according to the fact that because the MT stress of 600MPa in subloop is lower than the MT stress of 800MPa in full loop, the dislocations generated are small and thus the internal stress is small, resulting in a small decrease in the MT stress.

4.3.4. Deformation after cyclic loading. The stress-strain curves obtained by Exp. V are shown in Fig. 10. In Fig. 10, the path between the points A_i and D_i denotes the unloading process and the path between the points D_i and A_{i+1}– the reloading process. As seen in Fig. 10, MT starts at the point M_s and progresses to the point B_i through the unloading start point A_i. The reverse transformation

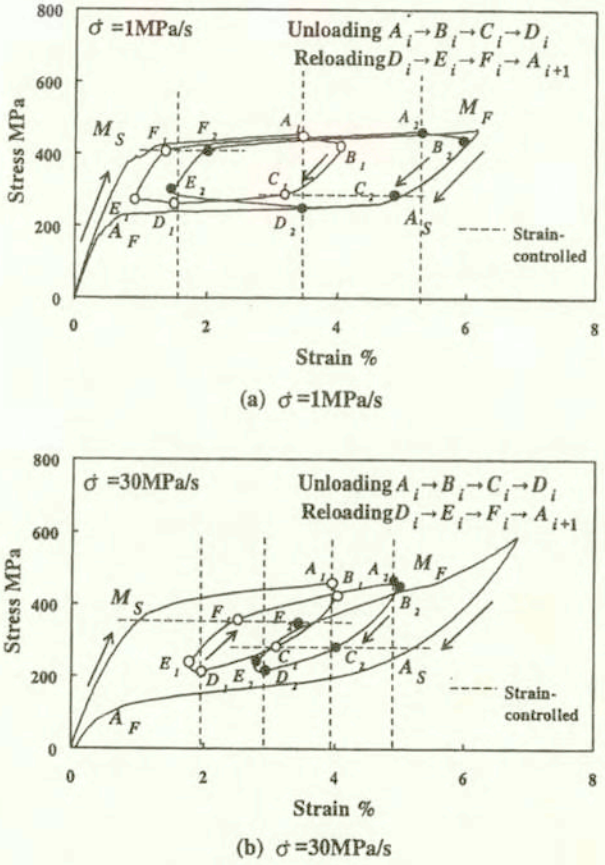

FIG. 10. Stress-strain curves under stress-controlled conditions after cyclic loading.

starts at the point C_i and progresses to the point E_i through the reloading start point D_i. As seen in Figs. 10(a) and (b), the higher is the stress rate, the higher is also the MT stress and the lower is the reverse transformation stress. This occurs according to the fact that if the stress rate is high, temperature of the material increases owing to MT, resulting in an increase in the MT stress and temperature of the material decreases owing to the reverse transformation, resulting

in a decrease in the reverse transformation stress. These deformation properties are similar to those without cyclic deformation shown in Fig. 6. In the case of subsequent subloop after cyclic loading, the condition for the transformation is stable, and therefore the stress levels at the points M_s and F_i and those at the points A_s and C_i, respectively, coincide.

5. Conclusions

The deformation properties of TiNi SMA subjected to strain control and stress control were investigated experimentally. The results obtained are summarized as follows. (1) In the case of a full loop, the stress-strain curves under stress-controlled conditions are similar to those under strain-controlled conditions with high strain rate. The overshoot and undershoot do not appear at the start points of SIMT in these curves. (2) In the case of a subloop under stress-controlled condition, temperature decreases and therefore the strain increases owing to the martensitic transformation at the early stage in the unloading process. At the early stage in the reloading process, temperature increases and therefore the strain decreases owing to the reverse transformation. (3) In the case of subloop under stress-controlled condition, the starting stresses of MT and the reverse transformation in the loading and unloading processes coincide with the transformation stresses under strain-controlled condition with low strain rate, respectively. (4) The deformation behaviors for subloop under stress-controlled condition are prescribed by the condition for progress of MT based on the transformation kinetics. (5) The deformation behavior subjected to cyclic loading under stress-controlled condition at constant temperature is also prescribed by the condition for progress of SIMT.

Acknowledgements

The experimental work of this study was carried out with the assistance of the students of Aichi Institute of Technology, to whom the authors wish to express their gratitude. The authors also want to extend their thanks to the Scientific Foundation of the Japanese Ministry of Education, Science, Sports and Culture for financial support.

References

1. H. FUNAKUBO, *Shape memory alloys*, Gordon and Break Science Pub., 1987.
2. T. DUERIG, K. MELTON, D. STOCKEL and C. WAYMAN [Eds.] *Engineering aspects of shape memory alloys*, Butterworth-Heinemann, 1990.

3. K. OTUKA and C.M. WAYMANN [Eds.] *Shape memory materials*, Cambridge University Press, 1998.

4. T. SABURI [Ed.] *Shape memory materials*, Trans Tech Pub., 2000.

5. J. A. SHAW and S. KYRIAKIDES, *Thermomechanical aspects of TiNi*, J. Mech. Phys. Solids, **43**, 8, 1243-1281, 1995.

6. H. TOBUSHI, Y. SHIMENO, T. HACHISUKA and K. TANAKA, *Influence of strain rate on superelastic properties of TiNi shape memory alloy*, Mech. Mater., **30**, 141-150, 1998.

7. G. SOCHA, B. RANIECKI AND S. MIYAZAKI, *Influence of control parameters on inhomogenity and the deformation behavior of Ti-51.0at%Ni SMA undergoing martensitic phase transformation at pure tension*, 33rd Solid Mechanics Conference, 369-370, 2000.

8. H. TOBUSHI, H. IWANGA, K. TANAKA, T. HORI and T. SAWADA, *Deformation behavior of TiNi shape memory alloy subjected to variable stress and temperature*, Continuum Mech. Thermodym., **3**, 79-93, 1991.

9. K. TANAKA, F. NISIMURA, T. HAYASHI, H. TOBUSHI and C. LEXCELLENT, *Phenomenological analysis on subloops and cyclic behavior in shape memory alloys under mechanical and/or thermal loads*, Mech. Mater., **19**, 281-292, 1995.

10. K. TANAKA, S. KOBAYASHI and Y. SATO, *Thermomechanics of transformation pseudoelasticity and shape memory effect in alloys*, Inter. J. Plasticity, **2**, 59-72, 1986.

11. K. TANAKA, *A Thermomechanical sketch of shape memory effects: one-dimensional tensile behavior*, Res Mechanica, **18**, 251-263, 1986.

12. H. TOBUSHI, K. TANAKA, K. KIMURA, T. HORI and T. SAWADA, *Stress-strain-temperature relationship associated with the R-phase transformation in TiNi shape memory alloy*, JSME Inter. J., I, **35**-3, 278-284, 1992.

13. S. MIYAZAKI, T. IMAI, Y. IGO and K. OTSUKA, *Effect of cyclic deformation on the pseudoelasticity characteristics of Ti-Ni alloys*, Metall. Trans. A, **17A**, 115-120, 1986.

14. H. TOBUSHI, S. YAMADA, T. HACHISUKA, A. IKAI and K. TANAKA, *Thermomechanical properties due to martensitic and R-phase transformations of TiNi shape memory alloy subjected to cyclic loadings*, Smart Mater. Struct., **5**, 788-795, 1996.

15. P.H. LIN, H. TOBUSHI, K. TANAKA, T. HATTORI and M. MAKITA, *Pseudoelastic behavior of TiNi shape memory alloy Subjected to Strain Variations*, J. Intelligent Mater. Systems Struct., **5**, 694-701, 1994.

16. S. P. GADAJ, W. K. NOWACKI and H. TOBUSHI, *Temperature evolution during tensile test of TiNi shape memory alloy*, Arch. Mech., **51**-6, 649-664, 1999.

Received May 25, 2001; revised version August 1, 2001.